How to Deploy RIS to Minimize Delay Spread in HST Communications: Railroad Side, or Train Side?

Ke Wang, Chan-Tong Lam, and Benjamin K. Ng
Faculty of Applied Sciences, Macao Polytechnic University
Macao S.A.R, China
Emails: {ke.wang; ctlam; bng}@ipm.edu.mo

***Abstract*—High-speed train (HST) communications are challenging due to fast time-varying channels and Doppler effects. Recently, reconfigurable intelligent surface (RIS) has been envisioned to be one of the most promising technologies for tackling the difficult problems of HST communications. In this paper, we first propose a transmission model of the HST communication system using RIS on the train side. Then, different strategies for mitigating delay spread (DS) are compared from the perspectives of the phase shift set design and deployment of the RIS. In addition, we derive the spectral efficiency (SE) expression of the proposed system. Numerical evaluations validate the analytical results and reveal that the RIS on the train side not only increases SE but also reduces DS.**

***Index Terms*—Reconfigurable intelligent surface, Doppler effect, delay spread, high-speed train communications, spectral efficiency**

I. Introduction

Reconfigurable intelligent surface (RIS), also known as intelligent reflecting surface, has become an innovative technique that allows control of the electromagnetic environment [1]. Recently, RIS has been envisioned to be a potential technology for high-speed train (HST) communication systems to achieve high spectral efficiency (SE) and energy efficiency [2]. In contrast to other wireless networks, the high mobility of the transceivers and the significant signal penetration loss passing through carriages characterize the HST communication. Consequently, many design difficulties, such as channel modeling, Doppler effect compensation, and time-varying channel estimation, arise as the results of these unique traits [3], [4].

There have already been some studies on RIS-assisted high-speed communications. In [5], the author revisited the multipath fading phenomenon in the context of RIS and showed that using real-time tunable RIS, the rapid fluctuations caused by the Doppler effect in received signal strength can be effectively mitigated. In [6], the authors introduced a general time-varying model for RIS-aided communication in the high-mobility scenario. The authors of [7] proposed to use positioning information such as GPS signals to design RIS phase shift sets, which helps to reduce the complexity of beamforming. Besides, the authors of [8] introduced a novel anti-Doppler technique in high-mobility vehicular communications using RIS, and it is shown that the roadside RIS can maximize the signal-to-noise ratio and mitigate Doppler spread simultaneously.

The above works [5]–[8] all considered the RIS next to the base station (BS), i.e., on the roadside. However, in the HST communication, the RIS can also be deployed on the vehicle side. Huang *et al.* [9] studied a high-speed communication system with the RIS deployed in a moving vehicle to assist its passenger's communication with the static BS on the roadside. The results showed that the RIS on the vehicle side can obtain high passive beamforming gain as well as convert the overall channel from fast to slow fading. Besides, Xu *et al.* [10] showed that improving the RIS-user link of the cascaded channel is more beneficial than that of the BS-RIS link. But both [9] and [10] did not consider the delay spread (DS) minimization, which is important to the HST communication [3], [4].

In this paper, we study the delay spread minimization using RIS on the train side in the HST communication. Our contributions are as follows:

- Different from the railroad side RIS, we first present a transmission model to accommodate the HST communication system using the RIS on the train side.
- Then, we compare different phase shift sets and deployment strategies for minimizing the DS.
- Lastly, the SE expression is derived for the proposed system.

Notation: Lower-case boldface letters denote the column vector. The function $(x \bmod y)$ refers to the remainder of the division of x by y. Superscript $[\cdot]^{\mathrm{T}}$ stands for transpose operation. Besides, $\lceil\cdot\rceil$ denotes the ceiling of the argument, $\lfloor\cdot\rfloor$ is the floor function, the set of positive integer set is denoted by $\mathbb{Z}_0^+$, $|\cdot|$ is the absolute value, $\jmath \triangleq \sqrt{-1}$, and $\|\cdot\|$ represents the l_2 norm.

II. System Model

We consider a downlink transmission model where an RIS consisting of $M \times N$ isotropic[1] reflecting elements is deployed on a HST to assist the communication from a static BS next

[1]Isotropic denotes the antenna gain of each element of the RIS is 1, i.e., it radiates equal signal power in all directions without antenna gain loss. A more practical non-isotropic case is left open for future work.

to the railroad to an in-train user with a speed v meters / second (m/s). The BS and the user both equip single isotropic antenna, and with the positions $\boldsymbol{p}_{\text{BS}} = [x_{\text{BS}}, h_{\text{BS}}, z_{\text{BS}}]^{\text{T}}$ and $\boldsymbol{p}_{\text{U}}(t) = [x_{\text{start}}+v \cdot t, h_{\text{U}}, z_{\text{U}}]^{\text{T}}$, respectively. Note that x_{start} is the starting point of the HST. As shown in Fig. 1, the RIS is a uniform planar array that is placed on a rectangular grid spaced dx and dy apart in the three-dimensional Cartesian coordinate system, and the heights of the RIS, the BS, and the user are h_{RIS}, h_{BS} and h_{U}, respectively. Furthermore, the channel state information (CSI) can be obtained via the methods proposed in [11] and [12][2], and the trajectory of the HST is along the x-axis direction.

The position vector of the (m, n)-th element on the RIS is

$$\bar{\boldsymbol{p}}_{m,n}(t) = \big[\omega(m, dx, M) + \Delta + x_{\text{start}} + v \cdot t, \\ \omega(n, dy, N) + h_{\text{RIS}}, z_{\text{U}}\big]^{\text{T}}, \quad (1)$$

where Δ is the distance between the user and the center of the RIS on the x-axis, and $\omega(m, dx, M) = dx(m - 0.5((M + 1) \bmod 2))$, $m \in \Omega(M)$ with

$$\Omega(M) = \left\{ \big((M+1) \bmod 2\big) - \left\lfloor \frac{M}{2} \right\rfloor, \dots, \left\lfloor \frac{M}{2} \right\rfloor \right\}, \quad (2)$$

and $\omega(n, dy, N)$ is obtained in the same way as $\omega(m, dx, M)$.

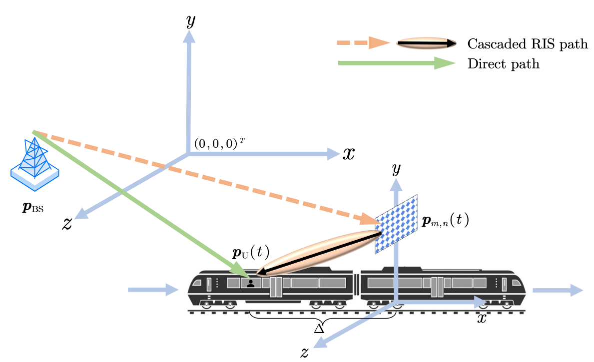

Fig. 1. An train side RIS aided HST communication system.

Since the RIS cannot reflect the signal to the user if it parallels the xoy plane, we rotate $\gamma \in [0, \pi/2]$ degrees in the opposite direction (i.e., counterclockwise direction) along the y-axis. Therefore, the practical position vector of the RIS is $\boldsymbol{p}_{m,n}(t) = \boldsymbol{\Gamma}^{\text{T}}(\gamma)\bar{\boldsymbol{p}}_{m,n}(t)$, where $\boldsymbol{\Gamma}(\gamma)$ is

$$\boldsymbol{\Gamma}(\gamma) = \begin{bmatrix} \cos(\gamma) & 0 & -\sin(\gamma) \\ 0 & 1 & 0 \\ \sin(\gamma) & 0 & \cos(\gamma) \end{bmatrix}. \quad (3)$$

Suppose the channels are all light-of-sight (LoS) [4], and small-scale fading is ignored. Then, at time t, the gain for the direct link between the BS and the user is

[2]If the mobility pattern is predicted (e.g., positioning information [7] and HST operation patterns [4], [8]), the CSI can be partly obtained in advance.

$$A_0(t) = \frac{\lambda_c}{4\pi \|\boldsymbol{p}_{\text{U}}(t) - \boldsymbol{p}_{\text{BS}}\|}, \quad (4)$$

where λ_c denotes the wavelength of the signal, and $\|\boldsymbol{p}_{\text{U}}(t) - \boldsymbol{p}_{\text{BS}}\|$ is the Euclidean distance between the BS and the user at time t. Also, the instantaneous gain of the (m, n)-th element of the RIS can be obtained as

$$A_{m,n}(t) = \frac{\lambda_c^2}{16\pi^2 \|\boldsymbol{p}_{m,n}(t) - \boldsymbol{p}_{\text{BS}}\| \|\boldsymbol{p}_{\text{U}}(t) - \boldsymbol{p}_{m,n}(t)\|}, \quad (5)$$

where $\|\boldsymbol{p}_{m,n}(t) - \boldsymbol{p}_{\text{BS}}\|$ and $\|\boldsymbol{p}_{\text{U}}(t) - \boldsymbol{p}_{m,n}(t)\|$ are the distances from the (m, n)-th element to the BS, and from the user to the (m, n)-th element, respectively. It is noteworthy that different from [5], [7], [10]–[12], the position of the RIS in this paper is related to the time t.

Besides, the time delays of the direct link and cascaded link at time t are

$$\tau_0(t) = \frac{\|\boldsymbol{p}_{\text{U}}(t) - \boldsymbol{p}_{\text{BS}}\|}{c_0}, \quad (6)$$

and

$$\tau_{m,n}(t) = \frac{\|\boldsymbol{p}_{m,n}(t) - \boldsymbol{p}_{\text{BS}}\| + \|\boldsymbol{p}_{\text{U}}(t) - \boldsymbol{p}_{m,n}(t)\|}{c_0}, \quad (7)$$

respectively. If $\phi_{m,n}(t) \in (0, 2\pi]$ denotes the phase shift of the (m, n)-th element on the RIS, $\Theta_0(t) \triangleq e^{-\jmath 2\pi f_c \tau_0(t)}$ and $\Theta_{m,n}(t) \triangleq e^{-\jmath 2\pi f_c \tau_{m,n}(t) - \jmath \phi_{m,n}(t)}$ are the phase part of the direct and the cascaded links, respectively. Thus the received signal can be obtained as

$$y(t) = S_0(t)\Theta_0(t) + \sum_{m=1,n=1}^{M,N} S_{m,n}(t)\Theta_{m,n}(t) + w, \quad (8)$$

where

$$S_0(t) = A_0(t)\left\{\sqrt{P_t}x(t - \tau_0(t))\right\}, \quad (9)$$

and

$$S_{m,n}(t) = A_{m,n}(t)\left\{\sqrt{P_t}x(t - \tau_{m,n}(t) - \frac{\phi_{m,n}(t)}{2\pi f_c})\right\}. \quad (10)$$

Note that $x(t)$ is the transmit signal with $\mathbb{E}\{|x(t)|^2\} = 1$, P_t is transmit power, f_c is carrier frequency, and w is a white Gaussian noise process with power spectral density N_0. We don't consider hardware impairments (HWI) in this paper[3].

III. Delay Spread Mitigation

In this section, we first give the expression for the DS of the RIS-assisted HST communication system. Then, we minimize the DS by optimizing the phase shift set and the deployment of the RIS.

[3]When considering HWI, the Doppler spread still can be almost removed by the RIS. However, the delay spread may increase when the RIS HWI becomes severe [7], [13].

A. Delay Spread Expression

The DS of the RIS-assisted high-speed communication system is defined as the maximum propagation time difference over the direct and cascaded paths [8], i.e., $T(t) = \max\{T_0(t), T_{\mathrm{RIS}}(t)\}$. Note that $T_0(t)$ is the DS between the direct path and the RIS which can be expressed as

$$T_0(t) = \max_{m,n}\left\{\tau_{m,n}(t) + \frac{\phi_{m,n}(t)}{2\pi f_c}\right\} - \tau_0(t), \tag{11}$$

and $T_{\mathrm{RIS}}(t)$ is the DS across the RIS itself, which is defined as follow

$$T_{\mathrm{RIS}}(t) = \max_{m,n}\left\{\tau_{m,n}(t) + \frac{\phi_{m,n}(t)}{2\pi f_c}\right\} - \min_{m',n'}\left\{\tau_{m',n'}(t) + \frac{\phi_{m',n'}(t)}{2\pi f_c}\right\}. \tag{12}$$

Since $\tau_0(t) < \min\{\tau_{m,n}(t) + \frac{\phi_{m,n}(t)}{2\pi f_c}\}$, then $T_0(t) > T_{\mathrm{RIS}}(t)$. Therefore, $T(t) = \max\{T_0(t), T_{\mathrm{RIS}}(t)\} = T_0(t)$.

It has been proved that the RIS can maximize the received power and remove the Doppler spread [6], [7], and the optimized phase shift set is

$$\phi^*_{m,n}(t) = 2\pi\left\{f_c\big(\tau_0(t) - \tau_{m,n}(t)\big) + k_{m,n}(t)\right\}, \tag{13}$$

where $k_{m,n}(t) \in \mathbb{Z}_0^+$, and larger or equals to $f_c(\tau_{m,n}(t) - \tau_0(t))$. Specifically, since $(\tau_0(t) - \tau_{m,n}(t)) < 0$, $\phi^*_{m,n}(t)$ should contains extra full carrier delay $2\pi k_{m,n}(t)$ to ensure the final phase shift range is $(0, 2\pi]$. By doing so, the Doppler spread can be removed, although the Doppler shift still exists.

B. Delay Spread Mitigation on Phase Shift Set

Using (13), we then have

$$\begin{aligned} T(t) &= \max_{m,n}\left\{\tau_{m,n}(t) + \frac{\phi^*_{m,n}(t)}{2\pi f_c}\right\} - \tau_0(t) \\ &= \frac{1}{f_c}\max_{m,n}\left\{k_{m,n}(t)\right\}. \end{aligned} \tag{14}$$

Thus, the DS mitigation problem can be obtained as follow

$$\text{(P1)}: \min_{k_{m,n}(t)} \frac{1}{f_c}\max_{m,n}\left\{k_{m,n}(t)\right\} \tag{15}$$

$$\text{s.t.} \quad k_{m,n}(t) \geq \lceil f_c(\tau_{m,n}(t) - \tau_0(t))\rceil, \tag{16}$$

Based on (14), if we want to minimize $T(t)$, the $k_{m,n}(t)$ should be as small as possible. Therefore, the solution of $(P1)$ is $k^{\mathrm{opt}}_{m,n}(t) = \lceil f_c(\tau_{m,n}(t) - \tau_0(t))\rceil$. Finally, the optimized phase shift is

$$\phi^{\mathrm{opt}}_{m,n}(t) = 2\pi\left\{f_c\big(\tau_0(t) - \tau_{m,n}(t)\big) + k^{\mathrm{opt}}_{m,n}(t)\right\}. \tag{17}$$

C. Delay Spread Mitigation on Deployment

Based on (17), the DS $T(t)$ can be obtained as

$$T(t) = \frac{1}{f_c}\max_{m,n}\left\{\lceil f_c(\tau_{m,n}(t) - \tau_0(t))\rceil\right\}. \tag{18}$$

So if we want to minimize $T(t)$ further, then $(\tau_{m,n}(t) - \tau_0(t))$ should be minimized. Recall (6) and (7), we have

$$\begin{aligned} \tau_{m,n}(t) - \tau_0(t) = &\frac{\|\boldsymbol{p}_{m,n}(t) - \boldsymbol{p}_{\mathrm{BS}}\| + \|\boldsymbol{p}_{\mathrm{U}}(t) - \boldsymbol{p}_{m,n}(t)\|}{c_0} \\ &- \frac{\|\boldsymbol{p}_{\mathrm{U}}(t) - \boldsymbol{p}_{\mathrm{BS}}\|}{c_0}. \end{aligned} \tag{19}$$

It is important to note that we cannot increase the direct link distance $\|\boldsymbol{p}_{\mathrm{U}}(t) - \boldsymbol{p}_{\mathrm{BS}}\|$ since this will cause a higher path loss. However, we can reduce the distance of the cascaded link instead. For the railroad side RIS case, the variation distance of the cascaded link is the RIS-user part [8]. Note that the relative distance between the static RIS and the high-mobility user changes rapidly, which causes high variations in channel phases and also results in a severe misalignment between direct and cascaded links. Therefore, if the RIS-user distance is fixed and small, then not only does the path loss decrease, but also the channel can become quasi-static. Given these reasons, deploying the RIS on the train is a better choice. Accordingly, $\|\boldsymbol{p}_{\mathrm{U}}(t) - \boldsymbol{p}_{m,n}\|$ becomes $\|\boldsymbol{p}_{\mathrm{U}}(t) - \boldsymbol{p}_{m,n}(t)\|$, which is almost a constant value during the operation time of the HST. Another reason is that the BS-RIS distance in the railroad side RIS case is often larger than the RIS-user distance in the train side RIS case [4]. Thus, a smaller path loss can be obtained in the latter case.

Given the reasons above, from the deployment perspective, the RIS should be deployed on the vehicle side. Table I compares and summarizes three different strategies.

IV. Spectral Efficiency Analysis

In this section, we derive the SE expression of the proposed system. In order to compute the SE, we use the phase shift set $\phi^{\mathrm{opt}}_{m,n}(t)$ in (17). Using this shift set, we can obtain the SE as follow

$$\begin{aligned} \mathrm{SE}(t) &= \mathbb{E}\left\{\log_2\left\{1 + \frac{|y(t) - w|^2}{N_0}\right\}\right\} \\ &= \log_2\left\{1 + \frac{\mathcal{Q}}{N_0}\right\}, \end{aligned} \tag{20}$$

where

TABLE I
Comparison between different DS minimization strategies.

Strategy	Phase Shift Set	Deployment
(13)	CANNOT $\min\{T(t)\}$	N/A
(17), Railroad Side	CAN $\min\{T(t)\}$	CANNOT $\min\{T(t)\}$
(17), HST Side	CAN $\min\{T(t)\}$	CAN $\min\{T(t)\}$

$$\mathcal{Q} = \mathbb{E}\{|y(t) - w|^2\} = P_t \Bigg\{ A_0^2(t) + A^\star(t) + \sum_{m=1,n=1}^{M,N} A_{m,n}^2(t) + 2A_0(t) \sum_{m=1,n=1}^{M,N} A_{m,n}(t) \Bigg\}, \tag{21}$$

and

$$A^\star(t) = A_1(t) \sum_{k \neq 1}^{MN} A_k(t) + A_2(t) \sum_{k \neq 2}^{MN} A_k(t) + \cdots + A_{MN}(t) \sum_{k \neq MN}^{MN} A_k(t). \tag{22}$$

Note that $k = 1, \ldots, MN$, and we use $\mathbb{E}\{\log_2(1 + x/y)\} \approx \log_2(1 + \mathbb{E}\{x\}/\mathbb{E}\{y\})$ [7] in (20) to approximate.

Special Case: If each element of the RIS is with nearly the same gain A_1, we then have

$$\mathrm{SE}_{A_1}(t) \approx \log_2 \left\{ 1 + \frac{\hat{\mathcal{Q}}}{N_0} \right\}, \tag{23}$$

where

$$\hat{\mathcal{Q}} \approx P_t \Bigg\{ A_0^2(t) + A_1^2(t)(MN)^2 + 2A_0(t)A_1(t)MN \Bigg\}. \tag{24}$$

Remark: If the direct link is blocked, then the received power $A_1^2(t)(MN)^2$ is proportional to $(MN)^2$, which is consistent with the square power law of the RIS-aided communication system [14].

V. Simulation Results and Discussions

In this section, numerical examples are provided to validate the results in Sections III and IV. We assume the BS is located at [0 m, h_{BS} m, 20 m]$^{\mathrm{T}}$, and the user in the HST locates at $[x_{\mathrm{start}} + v \cdot t$ m, h_{U} m, 50 m$]^{\mathrm{T}}$ where $t \in \mathbb{Z}_0^+$ and its range is from 1 s to 100 s. Two benchmarks are used, i.e., without RIS and RIS on the railroad side [8]. Note that the position of RIS in the latter case is[4] $\boldsymbol{p}_{m,n} = [\omega(m, a, M), \omega(n, b, N) + h_{\mathrm{RIS}}, 0]^{\mathrm{T}}$. Besides, since the elements of the RIS in this paper is isotropic, the area of each one should be adapted to the carrier frequency f_c [7]. Related parameters are shown in Table II.

TABLE II
Simulation Parameters [8], [15]

Parameters	Values
BS height (h_{BS})	20 m
RIS height (h_{RIS})	3 m
User height (h_{U})	1.5 m
Distance between the user and the center of the RIS (Δ)	3 m
Speed of the vehicle (v)	55 m/s
Start point of the vehicle (x_{start})	-5000 m
Total time	200 s
Transmit power (P_t)	20 dBm
Power spectral density (N_0)	-80 dBm/Hz
Carrier frequency (f_c)	2.4 GHz
The number of elements on RIS ($M \times N$)	64 $\times$ 64
Rotate Angle (γ)	45°
Rectangular grid spacing of the RIS (dx, dy)	$\frac{\lambda_c}{2\sqrt{\pi}}$, $\frac{\lambda_c}{2\sqrt{\pi}}$

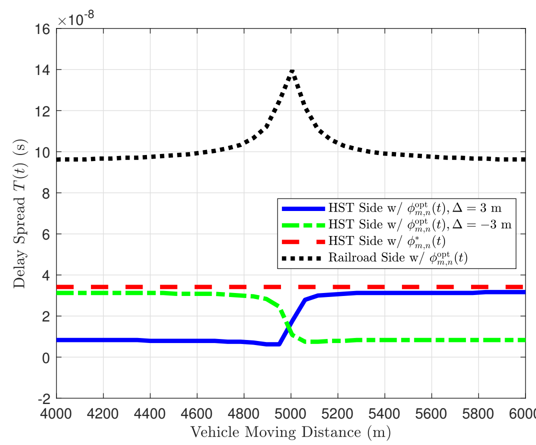

Fig. 2. Delay Spread for One Vehicle Pass.

Fig. 2 shows the effectiveness of the proposed DS minimization strategy. In particular, the case with phase shift $\phi_{m,n}^{\mathrm{opt}}(t)$ and the RIS on the HST side has the lowest DS, as expected. This is because in this case, the $k_{m,n}(t)$ can be optimized dynamically by the RIS, and the distance of the RIS-user link is shorter. Moreover, the case with phase shift $\phi_{m,n}^{*}(t)$ has a higher fixed delay spread. This is because the $k_{m,n}(t)$ in this case is a constant value. However, even the $k_{m,n}(t)$ is not optimized, the HST side RIS case with $\phi_{m,n}^{*}(t)$ still has a lower DS compared to the case that RIS on the railroad side and with the optimal phase shift $\phi_{m,n}^{\mathrm{opt}}(t)$. This result reveals that the appropriate deployment strategy of the RIS can significantly reduce the DS. Besides, if we change the locations of the user and the RIS, the changing pattern of the DS is different. In particular, if $\Delta = -3$ m, then the DS decreases when the HST passes by the BS. However, the HST side RIS case with $\phi_{m,n}^{\mathrm{opt}}(t)$ can always guarantee the lowest average DS.

Fig. 3 shows all SEs increase when the HST approaches the BS. This is because when the distances $\|\boldsymbol{p}_{\mathrm{U}}(t) - \boldsymbol{p}_{\mathrm{BS}}\|$ in (4) and $\|\boldsymbol{p}_{m,n}(t) - \boldsymbol{p}_{\mathrm{BS}}\|$ in (5) become small, the channel gains $A_0(t)$ and $A_{m,n}(t)$ increase. Furthermore, the highest point of all SEs is at around 5000 m. This is expected because, at this distance, the distance between the BS and the user is the smallest. In other words, $A_0(t)$ is the largest at this time. Besides, the HST side RIS case performs better than the case with the railroad side RIS. This is because when the RIS is on the HST side, the path attenuation decreases.

Fig. 4 shows the cumulative distribution function (CDF) of

[4]Note that normally h_{RIS} of the railroad side RIS case is higher than that of the train side RIS case, while we set the same height for the two cases in this paper for a fair comparison.

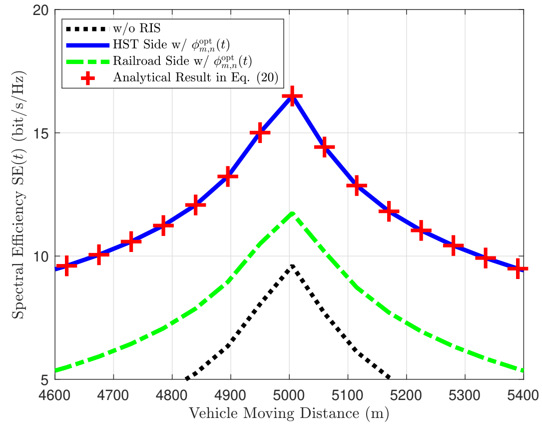

Fig. 3. Spectral Efficiency for One Vehicle Pass.

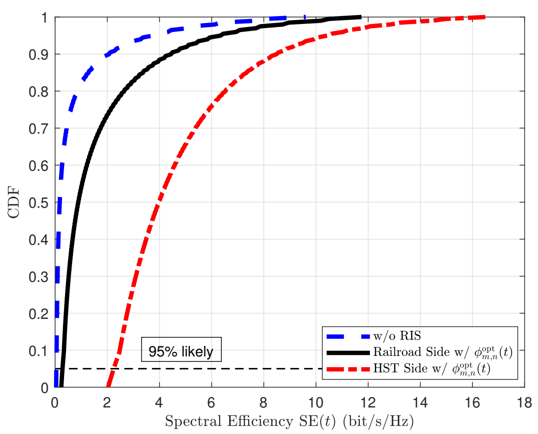

Fig. 4. CDF of Spectral Efficiency for One Vehicle Pass.

the SE for one vehicle pass. As expected, the RIS on the HST side performs the best. If we look at the 95% likely SE, indicated by the dashed line where the CDF value is 0.05, there is a 1.95 bit/s/Hz difference between the HST side and the railroad RIS. More precisely, the RIS on the HST side guarantees a SE of 2.23 bit/s/Hz (or higher) at 95%, while the RIS on the railroad side and without RIS only guarantee 0.28 and 0.04 bit/s/Hz, respectively.

It is worth noting that in practical scenarios, the system performance would also be affected by the rotation angle γ [16]. In particular, if the element is not isotropic, then there exists an optimal rotation angle that can maximize the antenna gain of the cascaded link. However, pursuing this maximized gain in this paper is challenging since 1) obtaining precise CSI is difficult, especially in high-speed communications, which makes γ inaccurate; 2) rotating the RIS would cost extra energy, which is not energy efficient. But in quasi-static scenarios, rotating RIS to obtain the extra degrees of freedom to optimize the system performance is possible [16].

VI. Conclusion

In this paper, we have minimized the delay spread of the RIS-assisted HST communication system by deploying the RIS on the train side. Besides, we have derived the SE expression of the proposed system. The simulation results have validated all the theoretical results. It has revealed that deploying the RIS on the train side can not only mitigate DS but also improve SE. A more practical case with Rician channels is left open for future work.

References

[1] C. Pan, H. Ren, K. Wang, J. F. Kolb, M. Elkashlan, M. Chen, M. Di Renzo, Y. Hao, J. Wang, A. L. Swindlehurst *et al.*, "Reconfigurable Intelligent Surfaces for 6G Systems: Principles, Applications, and Research Directions," *IEEE Communications Magazine*, vol. 59, no. 6, pp. 14–20, 2021.

[2] Y. Zhao, J. Zhang, and B. Ai, "Applications of Reconfigurable Intelligent Surface in Smart High Speed Train Communications," *arXiv preprint arXiv:2109.04354*, 2021.

[3] B. Ai, A. F. Molisch, M. Rupp, and Z.-D. Zhong, "5G Key Technologies for Smart Railways," *Proceedings of the IEEE*, vol. 108, no. 6, pp. 856–893, 2020.

[4] J. Zhang, H. Liu, Q. Wu, Y. Jin, Y. Chen, B. Ai, S. Jin, and T. J. Cui, "RIS-Aided Next-Generation High-Speed Train Communications: Challenges, Solutions, and Future Directions," *IEEE Wireless Communications*, vol. 28, no. 6, pp. 145–151, 2021.

[5] E. Basar, "Reconfigurable Intelligent Surfaces for Doppler Effect and Multipath Fading Mitigation," *Frontiers in Communications and Networks*, vol. 2, p. 14, 2021.

[6] E. Björnson, H. Wymeersch, B. Matthiesen, P. Popovski, L. Sanguinetti, and E. de Carvalho, "Reconfigurable Intelligent Surfaces: A signal processing perspective with wireless applications," *IEEE Signal Processing Magazine*, vol. 39, no. 2, pp. 135–158, 2022.

[7] K. Wang, C.-T. Lam, and B. K. Ng, "Positioning Information Based High-Speed Communications with Multiple RISs: Doppler Mitigation and Hardware Impairments," *Applied Sciences*, vol. 12, no. 14, p. 7076, 2022.

[8] ——, "IRS-Aided Predictable High-Mobility Vehicular Communication with Doppler Effect Mitigation," in *2021 IEEE 93rd Vehicular Technology Conference (VTC2021-Spring)*. IEEE, 2021, pp. 1–6.

[9] Z. Huang, B. Zheng, and R. Zhang, "Transforming Fading Channel from Fast to Slow: IRS-Assisted High-Mobility Communication," in *ICC 2021-IEEE International Conference on Communications*. IEEE, 2021, pp. 1–6.

[10] C. Xu, J. An, T. Bai, L. Xiang, S. Sugiura, R. G. Maunder, L.-L. Yang, and L. Hanzo, "Reconfigurable Intelligent Surface Assisted Multi-Carrier Wireless Systems for Doubly Selective High-Mobility Ricean Channels," *IEEE Transactions on Vehicular Technology*, 2022.

[11] W. Wu, H. Wang, W. Wang, and R. Song, "Doppler Mitigation Method Aided by Reconfigurable Intelligent Surfaces for High-Speed Channels," *IEEE Wireless Communications Letters*, vol. 11, no. 3, pp. 627–631, 2022.

[12] S. Sun and H. Yan, "Channel Estimation for Reconfigurable Intelligent Surface-Assisted Wireless Communications Considering Doppler Effect," *IEEE Wireless Communications Letters*, vol. 10, no. 4, pp. 790–794, 2020.

[13] K. Wang, C.-T. Lam, and B. K. Ng, "Doppler Effect Mitigation using Reconfigurable Intelligent Surfaces with Hardware Impairments," in *2021 IEEE Globecom Workshops (GC Wkshps)*. IEEE, 2021, pp. 1–6.

[14] Q. Wu and R. Zhang, "Intelligent Reflecting Surface Enhanced Wireless Network via Joint Active and Passive Beamforming," *IEEE Transactions on Wireless Communications*, vol. 18, no. 11, pp. 5394–5409, 2019.

[15] G. T. 38.913, "Technical Specification Group Radio Access Network; Study on Scenarios and Requirements for Next Generation Access Technologies;(Release 14)," *Tech. Rep.*, 2016.

[16] Y. Cheng, W. Peng, C. Huang, G. C. Alexandropoulos, C. Yuen, and M. Debbah, "RIS-Aided Wireless Communications: Extra Degrees of Freedom via Rotation and Location Optimization," *IEEE Transactions on Wireless Communications*, pp. 1–1, 2022.